



**University of  
Zurich<sup>UZH</sup>**

# Heavy $U$ -quark decay in the 4321-model

Master Thesis in Physics

Nando Zwahlen

Supervised by  
Prof. Dr. Gino Isidori

May 3, 2023

## Abstract

In this thesis the decay of a fourth generation  $U$ -quark was studied for a gauge model with a  $SU(4) \times SU(3) \times SU(2) \times U(1)$  symmetry and a fourth generation of heavy vector-like fermions. Under the assumption of small mass mixing and increasing masses for later generations, the leading order contribution of the 2-body and 3-body decay widths were computed in terms of the fundamental parameters. Finally, the two decay modes were compared for different mass values of the Leptoquark and the fourth generation  $U$ -quark.

## Acknowledgements

I want to thank Prof. Dr. Gino Isidori for the idea for this thesis and the introduction into the 4321-models. Furthermore, I want to thank him for always being helpful when I had questions concerning the physics behind the thesis.

# Contents

<b>I</b>	<b>Introduction</b>	<b>1</b>
<b>1</b>	<b>Motivation</b>	<b>1</b>
<b>2</b>	<b>Theory</b>	<b>2</b>
2.1	<i>SU</i> (4) and Leptoquarks . . . . .	2
2.2	The model . . . . .	3
<b>3</b>	<b>Procedure</b>	<b>4</b>
<b>II</b>	<b>Symmetry breaking and mass mixing</b>	<b>5</b>
<b>4</b>	<b>Symmetry breaking</b>	<b>5</b>
<b>5</b>	<b>Mass mixing</b>	<b>6</b>
5.1	Matrix perturbation theory . . . . .	7
5.2	Parameter reduction . . . . .	8
<b>III</b>	<b><i>U</i>-quark decay</b>	<b>9</b>
<b>6</b>	<b>Decay widths</b>	<b>10</b>
6.1	2-body decay . . . . .	10
6.2	3-body decay . . . . .	12
<b>7</b>	<b>The ratio <i>R</i></b>	<b>16</b>
<b>IV</b>	<b>Conclusions &amp; Outlook</b>	<b>18</b>

## List of Figures

1	Feynman diagrams of the $U$ -quark decay modes studied in this thesis. . . . .	4
2	Feynman diagram of a 6-dimensional EFT operator describing the $U$ -quark decay. . . . .	12
3	Schematic figure of the 3-body decay in the rest frame of the $U$ -quark. . . . .	14
4	R ratio as a function of the $U$ -quark mass for different LQ masses. . . . .	17

## List of Tables

1	Gauge representations of the fermions. . . . .	4
---	--	---

## Part I

# Introduction

## 1 Motivation

Pursuing the question of what this universe is made of and which laws it follows, there have been a large amount of discoveries made in particle physics in the last century. Most of these discoveries are embedded in the Standard Model (SM) of particle physics [1]. While the Standard Model is a full and conclusive theory itself, it fails to describe many physical phenomena and thus cannot be viewed as the fundamental theory of the interactions in the universe [2]. Besides the unification with general relativity and gravity, there are also phenomenological problems like the existence of neutrino masses, that cause neutrino oscillations [3]. Additionally, the fact that only a small amount of the energy spectrum has been measured in experiments leaves room for additional heavy particles besides the Standard Model particles. To study the emergence of new particles or interactions at high energies, many precision measurements have been performed using the high-energy particles from the Large Hadron Collider (LHC) [4]. One particularly interesting area for such precision tests is flavor physics. For all matter particles in the SM there are three identical copies, that only differ from each other in mass. For the leptonic sector there are no flavor changing vertices in the SM and the couplings to the gauge bosons are the same for all generations. This leads to a large sensitivity to new physics in lepton flavor non-universal processes. In the last years, several experiments have substantiated the inaccuracies of Standard Model predictions in the decay of B mesons [5]. The BABAR and LHCb collaborations are two of the most prominent examples for such experiments [6] [7]. While more data is taken in order to get statistically more significant results, the current knowledge about the semileptonic B decay is enough to spark a new interest in theories which have an additional mechanism of flavor-universality breaking. One specific group of models addressing this issue are the 4321 models, which have a  $SU(4) \times SU(3) \times SU(2) \times U(1)$  symmetry. These models originated from the Pati-Salam (PS) model, which tried to unify quark colors and leptons into a fourfold multiplet on which the  $SU(4)$  symmetry can act. The new results in B physics have excluded the Pati-Salam Leptoquark, as it is constrained to be heavy by flavor measurements ( $> 250\text{TeV}$ ) [8]. However, a Leptoquark would need to have a mass of a few TeV and a  $\mathcal{O}(1)$  coupling to the third generation fermions to explain the B anomalies, which excludes the original PS model [9]. In this thesis the decay of a fourth generation quark is studied for a specific 4321 model with a heavy vector-like fourth generation.

## 2 Theory

While the  $SU(3) \times SU(2) \times U(1)$  part is similar to the Standard Model and hence does not need an additional introduction, it is interesting to take a look at the  $SU(4)$  symmetry of the model.

### 2.1 $SU(4)$ and Leptoquarks

The  $SU(4)$  symmetry connects quark colors and leptons into a fourfold multiplet and interprets leptons as being the fourth color.

$$\psi_L = \begin{pmatrix} q_L^r \\ q_L^g \\ q_L^b \\ l_L \end{pmatrix} \quad \psi_R = \begin{pmatrix} q_R^r \\ q_R^g \\ q_R^b \\ l_R \end{pmatrix} \quad (1)$$

The gauge symmetry then has the following generators  $T_a^{SU(4)} = \frac{\lambda_a}{\sqrt{6}}$  with  $a = 1, 2, \dots, 15$  [10].

$$\begin{aligned} \lambda_1 &= \begin{pmatrix} 0 & 1 & 0 & 0 \\ 1 & 0 & 0 & 0 \\ 0 & 0 & 0 & 0 \\ 0 & 0 & 0 & 0 \end{pmatrix} & \lambda_2 &= \begin{pmatrix} 0 & -i & 0 & 0 \\ i & 0 & 0 & 0 \\ 0 & 0 & 0 & 0 \\ 0 & 0 & 0 & 0 \end{pmatrix} & \lambda_3 &= \begin{pmatrix} 1 & 0 & 0 & 0 \\ 0 & -1 & 0 & 0 \\ 0 & 0 & 0 & 0 \\ 0 & 0 & 0 & 0 \end{pmatrix} \\ \lambda_4 &= \begin{pmatrix} 0 & 0 & 1 & 0 \\ 0 & 0 & 0 & 0 \\ 1 & 0 & 0 & 0 \\ 0 & 0 & 0 & 0 \end{pmatrix} & \lambda_5 &= \begin{pmatrix} 0 & 0 & -i & 0 \\ 0 & 0 & 0 & 0 \\ i & 0 & 0 & 0 \\ 0 & 0 & 0 & 0 \end{pmatrix} & \lambda_6 &= \begin{pmatrix} 0 & 0 & 0 & 0 \\ 0 & 0 & 1 & 0 \\ 0 & 1 & 0 & 0 \\ 0 & 0 & 0 & 0 \end{pmatrix} \\ \lambda_7 &= \begin{pmatrix} 0 & 0 & 0 & 0 \\ 0 & 0 & -i & 0 \\ 0 & i & 0 & 0 \\ 0 & 0 & 0 & 0 \end{pmatrix} & \lambda_8 &= \frac{1}{\sqrt{3}} \begin{pmatrix} 1 & 0 & 0 & 0 \\ 0 & 1 & 0 & 0 \\ 0 & 0 & -2 & 0 \\ 0 & 0 & 0 & 0 \end{pmatrix} & \lambda_9 &= \begin{pmatrix} 0 & 0 & 0 & 1 \\ 0 & 0 & 0 & 0 \\ 0 & 0 & 0 & 0 \\ 1 & 0 & 0 & 0 \end{pmatrix} \\ \lambda_{10} &= \begin{pmatrix} 0 & 0 & 0 & -i \\ 0 & 0 & 0 & 0 \\ 0 & 0 & 0 & 0 \\ i & 0 & 0 & 0 \end{pmatrix} & \lambda_{11} &= \begin{pmatrix} 0 & 0 & 0 & 0 \\ 0 & 0 & 0 & 1 \\ 0 & 0 & 0 & 0 \\ 0 & 1 & 0 & 0 \end{pmatrix} & \lambda_{12} &= \begin{pmatrix} 0 & 0 & 0 & 0 \\ 0 & 0 & 0 & -i \\ 0 & 0 & 0 & 0 \\ 0 & i & 0 & 0 \end{pmatrix} \\ \lambda_{13} &= \begin{pmatrix} 0 & 0 & 0 & 0 \\ 0 & 0 & 0 & 0 \\ 0 & 0 & 0 & 1 \\ 0 & 0 & 1 & 0 \end{pmatrix} & \lambda_{14} &= \begin{pmatrix} 0 & 0 & 0 & 0 \\ 0 & 0 & 0 & 0 \\ 0 & 0 & 0 & -i \\ 0 & 0 & i & 0 \end{pmatrix} & \lambda_{15} &= \frac{1}{\sqrt{6}} \begin{pmatrix} 1 & 0 & 0 & 0 \\ 0 & 1 & 0 & 0 \\ 0 & 0 & 1 & 0 \\ 0 & 0 & 0 & -3 \end{pmatrix} \end{aligned} \quad (2)$$

Note that the first eight matrices  $\lambda_{1,2,\dots,8}$  form the subgroup  $SU(3)$  of  $SU(4)$  and can therefore be mixed with the pure  $SU(3)$  symmetry. The generators  $T_{9,\dots,14}$  facilitate an interaction between quarks and leptons, which can be described in the following way.

$$\begin{aligned} \mathcal{L} \supset -ig_4 \sum_{i=9}^{i=14} \bar{\psi} T_i \not{H}^i \psi &= -\frac{ig_4}{\sqrt{3}} \left( \bar{q}^r \not{U}^{1+l} + \bar{q}^g \not{U}^{2+l} + \bar{q}^b \not{U}^{3+l} + \bar{l} \not{U}^{1-r} q^r + \bar{l} \not{U}^{2-r} q^g + \bar{l} \not{U}^{3-r} q^b \right) \\ U_\mu^{1,2,3+} &= \frac{1}{\sqrt{2}} (H_\mu^{9,11,13} - iH_\mu^{10,12,14}) \\ U_\mu^{1,2,3-} &= \frac{1}{\sqrt{2}} (H_\mu^{9,11,13} + iH_\mu^{10,12,14}) \end{aligned} \quad (3)$$

These interaction vertices are particularly interesting, as they give rise to an additional flavor changing mechanism due to the misalignment of gauge and mass eigenstates.

Since the  $SU(4)$  symmetry of the 4321 models unifies quarks and leptons, the explanation of the different masses forces the existence of a new symmetry breaking mechanism. In this thesis the additional symmetry breaking is assumed to be at a larger scale than the relevant scale for fourth generation fermions decaying. Therefore, only true mass terms and mass terms stemming from the Higgs mechanism are regarded in this thesis.

## 2.2 The model

This chapter introduces a specific case of a 4321 model including a fourth generation of fermions, which is studied in this thesis. For further insights into the model one can see [9]. As expected for a 4321 theory, there are 4 different kinds of gauge fields:  $H_\mu^a$ ,  $C_\mu^b$ ,  $W_\mu^c$  and  $B'_\mu$  with indices  $a = 1, 2, \dots, 15$ ,  $b = 1, 2, \dots, 8$  and  $c = 1, 2, 3$ . While the  $SU(2)$  fields  $W_\mu^c$  are already the same as in the SM, the  $SU(4)$  and  $SU(3)$  mix, such that the SM gluons  $G_\mu^a$  and hypercharge bosons  $B_\mu$  are given by:

$$\begin{aligned} G_\mu^b &= c_3 \cdot C_\mu^b + s_3 \cdot H_\mu^b \\ B_\mu &= s_1 \cdot H_\mu^{15} + c_1 \cdot B'_\mu \end{aligned} \quad (4)$$

With  $b$  still being an index between 1 and 8 and  $s_1/c_1$  and  $s_3/c_3$  being the sine/cosine of the mixing angles  $\theta_1$  and  $\theta_3$ . Together with the Leptoquarks from equation 3, these are only 15 of the 24 gauge fields that are associated with  $SU(4)$ ,  $SU(3)$  and  $U(1)$ . The remaining gauge fields are given by:

$$\begin{aligned} G_\mu^{b'} &= -s_3 \cdot C_\mu^b + c_3 \cdot H_\mu^b \\ Z'_\mu &= -s_1 \cdot B'_\mu + c_1 \cdot H_\mu^{15} \end{aligned} \quad (5)$$

Again, the index  $b$  goes from 1 to 8. These gauge fields get masses through the spontaneous symmetry breaking  $SU(4) \times SU(3) \times U(1) \rightarrow SU(3)_C \times U(1)_Y$ .

Finally, it remains to introduce the fermion field content of the theory. As in the SM, there are three generations of quarks and leptons, but in this case the generations do not have the same gauge transformation properties. The first two generations have the same hypercharges and properties as in the SM, e.g. they are a singlet under  $SU(4)$  transformations. The third generation quarks transform as a singlet under  $SU(3)$  and in the fundamental representation of  $SU(4)$ , the same behavior as the third generation leptons. Additionally, there is a right-handed neutrino that is introduced for the third generation. For the fourth generation, vector like fermions are introduced. In this thesis the model 1 of [9] is used.

The fields with index  $i=1,2$  correspond to the first two generations. It is also noteworthy that all these fields are denoted in their gauge eigenstates. The third generation is given by the  $\psi$  fields:  $\psi_L = (q_L^3, l_L^3)^T$ ,  $\psi_R^{up-type} = (u_R^3, \nu_R^3)^T$  and  $\psi_R^{down-type} = (d_R^3, e_R^3)^T$ . Lastly, there is also the new heavy generation represented by large letters:  $Q_{L/R} = (U_{R/L}, D_{R/L})^T$  and  $L_{L/R} = (N_{R/L}, E_{R/L})^T$ .

Field	$SU(4)$	$SU(3)$	$SU(2)$	$U(1)$
$q_L^i$	1	3	2	1/6
$u_R^i$	1	3	1	2/3
$d_R^i$	1	3	1	-1/3
$l_L^i$	1	1	2	-1/2
$e_R^i$	1	1	1	-1
$\psi_L$	4	1	2	0
$\psi_R^{up-type}$	4	1	1	1/2
$\psi_R^{down-type}$	4	1	1	-1/2
$Q_L$	4	1	2	0
$Q_R$	1	3	2	1/6
$L_L$	4	1	2	0
$L_R$	1	1	2	-1/2

Table 1: Summary of the fermion fields and their representations in the gauge symmetries.

### 3 Procedure

In this thesis the decay of the fourth generation  $U$ -quark into SM particles is studied. This decay can happen through two different interaction types. First, there is the two-body decay into a  $W$ -boson and a bottom quark. Additionally, the Leptoquark can facilitate the decay  $U \rightarrow \nu\tau b$ .

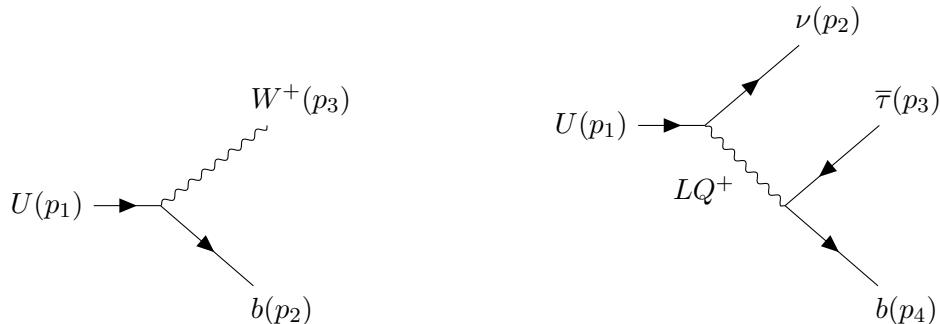


Figure 1: Feynman diagrams of the  $U$ -quark decay modes studied in this thesis.

For the  $U$ -quark decay one can define a ratio  $R$  between the two decay widths.

$$R = \frac{\Gamma(U \rightarrow W^+b)}{\Gamma(U \rightarrow \nu\tau b)} \tag{6}$$

The goal of this thesis is to study this ratio and express it in terms of the new mass parameters, which involve the fourth generation quarks.



## Part II

## Symmetry breaking and mass mixing

## 4 Symmetry breaking

In this section the symmetry breaking of the model is computed with the goal of finding the mixing angles as a function of the gauge couplings. The starting point for this is the kinetic part of the Lagrangian with its covariant derivative.

$$\begin{aligned}
\mathcal{L} \supset & \sum_{\psi=q_L^i, u_R^i, d_R^i, l_L^i, e_R^i, \psi_L, \psi_R^+, \psi_R^-, Q_L, Q_R, L_L, L_R} \bar{\psi} \not{\partial} \psi - i g_4 \sum_{\psi=\psi_L, \psi_R^+, \psi_R^-, Q_L, L_L} \bar{\psi} \not{H}^a T_a^{SU(4)} \psi \\
& - i g_3 \sum_{\psi=q_L^i, u_R^i, d_R^i, Q_R} \bar{\psi} \not{C}^b \bar{\lambda}^b \psi - i g_2 \sum_{\psi=q_L^i, l_L^i, \psi_L, Q, L} \bar{\psi} \not{W}^c \frac{\sigma^c}{2} \psi - i g_1 \sum_{\psi=q_L^i, u_R^i, d_R^i, l_L^i, e_R^i, \psi_R^+, \psi_R^-, Q_R, L_R} \bar{\psi} \not{B}' X_i \psi
\end{aligned} \tag{7}$$

$T_a^{SU(4)}$ , the Gell-Mann matrices  $\bar{\lambda}^b$  and the halved Pauli matrices  $\frac{\sigma^c}{2}$  are the generators of  $SU(4)$ ,  $SU(3)$  and  $SU(2)$  respectively. The charges  $X_i$  for  $U(1)$  can be distinct for different fields and are shown in table 1. This can be rewritten in a form such that the gauge fields that represent intact symmetries after the symmetry breaking are more clearly visible. Thus, the angles  $\theta_1$  and  $\theta_3$  can be derived. In equation 4, a general mixing of the  $SU(4)$  and  $SU(3)$  fields has already been assumed. The equations 4 and 5 can be transformed such that the initial gauge fields  $C_\mu^b$  and  $H_\mu^b$  are given as functions of the gauge fields  $G_\mu^b$  and  $G_\mu^{b'}$ . Plugging these relations into equation 7 and leaving out insignificant parts, yields:

$$\begin{aligned}
\mathcal{L} \supset & -i \left( g_4 \sum_{\psi=\psi_L, \psi_R^+, \psi_R^-, Q_L, L_L} \bar{\psi} T^b (c_3 G^{b'} + s_3 G^b) \psi + g_4 \sum_{\psi=\psi_L, \psi_R^+, \psi_R^-, Q_L, L_L} \bar{\psi} T^{15} (c_1 \not{Z}' + s_1 \not{B}) \psi \right. \\
& \left. + g_3 \sum_{\psi=q_L^i, u_R^i, d_R^i, Q_R} \bar{\psi} T^b (-s_3 G^{b'} + c_3 G^b) \psi + g_1 \sum_{\psi=q_L^i, u_R^i, d_R^i, l_L^i, e_R^i, \psi_R^+, \psi_R^-, Q_R, L_R} \bar{\psi} X_i (c_1 \not{B} - s_1 \not{Z}') \psi \right)
\end{aligned} \tag{8}$$

Here  $A_\mu$  represents the photon field.

To have the same behaviour for the strong gauge boson  $G_\mu^b$  as in the SM, the first three generation must have the same coupling strength. But one has to be careful, since the  $SU(4)$  generators have an additional factor  $\frac{1}{\sqrt{6}}$  in comparison to the Gell-Mann matrices.

$$g_S^{SM} = \frac{g_4 s_3}{\sqrt{6}} = g_3 c_3 \iff \tan(\theta_3) = \frac{g_3 \sqrt{6}}{g_4} \tag{9}$$

Before the analysis is continued, it is useful to introduce a notation that is better suited to discuss flavor. Since the goal of this thesis is to discuss the decaying behavior of the fourth generation, the first generation is neglected in this thesis from this point on. Aware that particles with different quantum numbers are mixed into the same vector, the following multiplets are

introduced:

$$\begin{aligned} u'_L = \begin{pmatrix} u_L^2 \\ u_L^3 \\ U'_L \end{pmatrix} d'_L = \begin{pmatrix} d_L^2 \\ d_L^3 \\ D'_L \end{pmatrix} u'_R = \begin{pmatrix} u_R^3 \\ U'_R \end{pmatrix} d'_R = \begin{pmatrix} d_R^3 \\ D'_R \end{pmatrix} \\ e'_L = \begin{pmatrix} e_L^2 \\ e_L^3 \\ E'_L \end{pmatrix} \nu'_L = \begin{pmatrix} \nu_L^2 \\ \nu_L^3 \\ N'_L \end{pmatrix} e'_R = \begin{pmatrix} e_R^3 \\ E'_R \end{pmatrix} \nu'_R = \begin{pmatrix} \nu_R^3 \\ N'_R \end{pmatrix} \end{aligned} \quad (10)$$

The left-handed fields  $q_L$  and  $l_L$  are defined as:

$$q'_L = \left( \begin{pmatrix} u_L^2 \\ d_L^2 \end{pmatrix}, \begin{pmatrix} u_L^3 \\ d_L^3 \end{pmatrix}, \begin{pmatrix} U'_L \\ D'_L \end{pmatrix} \right)^T \quad l'_L = \left( \begin{pmatrix} \nu_L^2 \\ e_L^2 \end{pmatrix}, \begin{pmatrix} \nu_L^3 \\ e_L^3 \end{pmatrix}, \begin{pmatrix} N'_L \\ E'_L \end{pmatrix} \right)^T \quad (11)$$

The terms involving the SM gauge field  $B_\mu$  of equation 8 can then be rewritten, while leaving out the first generation particles as already mentioned.

$$\begin{aligned} \mathcal{L} \supset -i[\bar{q}'_L \text{diag}(\frac{g_1}{6}c_1\mathcal{B}, \frac{g_4}{\sqrt{6}}s_1\mathcal{B}, \frac{g_4}{\sqrt{6}}s_1\mathcal{B})q'_L + \bar{l}'_L \text{diag}(-\frac{g_1}{2}c_1\mathcal{B}, -\frac{3g_4}{\sqrt{6}}s_1\mathcal{B}, -\frac{3g_4}{\sqrt{6}}s_1\mathcal{B})l'_L + \\ \bar{u}'_R \text{diag}(\frac{g_4}{\sqrt{6}}s_1\mathcal{B} + \frac{g_1}{2}c_1\mathcal{B}, \frac{g_1}{6}c_1\mathcal{B})u'_R + \bar{d}'_R \text{diag}(\frac{g_4}{\sqrt{6}}s_1\mathcal{B} - \frac{g_1}{2}c_1\mathcal{B}, \frac{g_1}{6}c_1\mathcal{B})d'_R + \\ \bar{e}'_R \text{diag}(-\frac{3g_4}{\sqrt{6}}s_1\mathcal{B} - \frac{g_1}{2}c_1\mathcal{B}, -\frac{g_1}{2}c_1\mathcal{B})e'_R + \bar{\nu}'_R \text{diag}(-\frac{3g_4}{\sqrt{6}}s_1\mathcal{B} + \frac{g_1}{2}c_1\mathcal{B}, -\frac{g_1}{2}c_1\mathcal{B})\nu'_R] \end{aligned} \quad (12)$$

The mixing angle  $\theta_1$  can be found by requiring that the couplings of the fermion fields to the gauge field  $B_\mu$  are the same as in the SM for the first three generations.

$$\begin{aligned} q'_L : \frac{g'_{SM}}{6} = \frac{g_1}{6}c_1 = \frac{g_4}{\sqrt{6}}s_1 \\ l'_L : -\frac{g'_{SM}}{2} = -\frac{g_1}{2}c_1 = -\frac{3g_4}{\sqrt{6}}s_1 \\ u'_R : \frac{2}{3}g'_{SM} = \frac{2}{3}g_1c_1 = \frac{g_4}{\sqrt{6}}s_1 + \frac{g_1}{2}c_1 \\ d'_R : -\frac{1}{3}g'_{SM} = -\frac{1}{3}c_1g_1 = \frac{g_4}{\sqrt{6}}s_1 - \frac{g_1}{2}c_1 \\ e'_R : -g'_{SM} = -g_1c_1 = -\frac{3g_4}{\sqrt{6}}s_1 - \frac{g_1}{2}c_1 \end{aligned} \quad (13)$$

All these equations give the same value for the angle  $\theta_1$  and for  $g'_{SM}$  and thus a consistent symmetry breaking pattern is achieved.

$$\begin{aligned} g'_{SM} = g_1c_1 = \sqrt{6}g_4s_1 \\ \tan(\theta_1) = \frac{g_1}{g_4\sqrt{6}} \end{aligned} \quad (14)$$

## 5 Mass mixing

Before the Feynman rules can be calculated, it is important to recollect that up to this point the formulas were written in the gauge eigenstates of the fields. As already stated, the additional symmetry breaking mechanism that is used to give leptons distinct masses from the quarks in

$SU(4)$  is neglected, as in this thesis scales below this mechanism are interesting. Therefore, only Yukawa interactions and real mass terms are looked at.

$$\mathcal{L} \supset \bar{u}'_L \begin{pmatrix} \lambda_{23}^u \frac{v}{\sqrt{2}} & 0 \\ \lambda_{33}^u \frac{v}{\sqrt{2}} & m'_q \\ \Lambda^u \frac{v}{\sqrt{2}} & M'_q \end{pmatrix} u'_R + \bar{d}'_L \begin{pmatrix} \lambda_{23}^d \frac{v}{\sqrt{2}} & 0 \\ \lambda_{33}^d \frac{v}{\sqrt{2}} & m'_q \\ \Lambda^d \frac{v}{\sqrt{2}} & M'_q \end{pmatrix} d'_R + \bar{e}'_L \begin{pmatrix} \lambda_{23}^e \frac{v}{\sqrt{2}} & 0 \\ \lambda_{33}^e \frac{v}{\sqrt{2}} & m'_l \\ \Lambda^e \frac{v}{\sqrt{2}} & M'_l \end{pmatrix} e'_R + \bar{\nu}'_L \begin{pmatrix} \lambda_{23}^\nu \frac{v}{\sqrt{2}} & 0 \\ \lambda_{33}^\nu \frac{v}{\sqrt{2}} & m'_l \\ \Lambda^\nu \frac{v}{\sqrt{2}} & M'_l \end{pmatrix} \nu'_R \quad (15)$$

Without knowing their values, a set of fields in the mass eigenstate are defined:

$$u_L = \begin{pmatrix} c_L \\ t_L \\ U_L \end{pmatrix} d_L = \begin{pmatrix} s_L \\ b_L \\ D_L \end{pmatrix} u_R = \begin{pmatrix} t_R \\ U_R \end{pmatrix} d_R = \begin{pmatrix} b_R \\ D_R \end{pmatrix} \\ e_L = \begin{pmatrix} \mu_L \\ \tau_L \\ E_L \end{pmatrix} \nu_L = \begin{pmatrix} \nu_L^\mu \\ \nu_L^\tau \\ N_L \end{pmatrix} e_R = \begin{pmatrix} \tau_R \\ E_R \end{pmatrix} \nu_R = \begin{pmatrix} \nu_R^\tau \\ N_R \end{pmatrix} \quad (16)$$

The mixing matrices  $Y^i$  from equation 15 are diagonalized using the unitary matrices  $(W_L^i)_{3 \times 3}$  and  $(W_R^i)_{2 \times 2}$ , with the index  $i = u, d, e, \nu$  corresponding to the particle type.

$$Y_{diag}^i = W_L^{i\dagger} Y^i W_R^i \\ (Y^{i\dagger} Y^i)_{diag} = W_R^{i\dagger} (Y^{i\dagger} Y^i) W_R^i \\ (Y^i Y^{i\dagger})_{diag} = W_L^{i\dagger} (Y^i Y^{i\dagger}) W_L^i \quad (17)$$

## 5.1 Matrix perturbation theory

To calculate the mixing matrices between the gauge and the mass eigenstates, matrix perturbation theory is used. For this it is assumed that the matrix, that should be diagonalized, only has small off-diagonal elements and can be diagonalized to each order by a unitary mixing matrix.

$$M = M_0^{diag} + \epsilon M_1^{off-diag} \\ W = W_0 + \epsilon W_1 + \epsilon^2 W_2 + \mathcal{O}(\epsilon^3) \quad (18)$$

At  $\mathcal{O}(\epsilon^0)$  one gets  $W_0 = I$ , such that  $W_0$  is unitary and keeps  $M_0$  diagonal. Up to order  $\mathcal{O}(\epsilon)$  it gets more interesting:

$$W^\dagger W = I + \epsilon(W_1 + W_1^\dagger) = I \\ \Rightarrow W_1 = -W_1^\dagger \\ W^\dagger M W = M_0 + \epsilon(M_1 + M_0 W_1 + W_1^\dagger M_0) \\ \Rightarrow M_1 = [W_1, M_0] \quad (19)$$

Note that these formulae are for quadratic matrices and that there is no correction to the diagonal elements of  $M$  at this order. Now the mixing matrices  $W_R^i$  and  $W_L^i$  can be computed up to first order using the equations from 17.

$$Y^{i\dagger} Y^i = \begin{pmatrix} \frac{v^2}{2} (|\lambda_{23}^i|^2 + |\lambda_{33}^i|^2 + |\Lambda^i|^2) & \frac{v}{\sqrt{2}} (m \lambda_{33}^{i*} + M \Lambda^{i*}) \\ \frac{v}{\sqrt{2}} (m^* \lambda_{33}^i + M^* \Lambda^i) & m^2 + M^2 \end{pmatrix} \quad (20)$$

To use the matrix perturbation framework, a look at the hierarchy of the scales in our theory is needed. Assuming a similar hierarchy as in the SM, small mixing and increasingly heavier generations lead to the hierarchy  $M \gg v, m$ . By factoring out  $M^2$ , it is now obvious that

there are  $\mathcal{O}(1)$  elements in the diagonal and  $\mathcal{O}(\frac{v}{M})$  elements in the off-diagonal. Thus, matrix perturbation theory is applicable and the last equation of 19 can be used to get the mixing matrix (in this case the equation is multiplied by  $\epsilon$ ).

$$W_R^i = \begin{pmatrix} 1 & W_{12}^{R,i} \\ -W_{12}^{R,i*} & 1 \end{pmatrix} \quad (21)$$

$$W_{12}^{R,i} = \frac{\frac{v}{\sqrt{2}}(m\lambda_{33}^{i*} + M\Lambda^{i*})}{m^2 + M^2 - \frac{v^2}{2}(|\lambda_{23}^i|^2 + |\lambda_{33}^i|^2 + |\Lambda^i|^2)}$$

The  $3 \times 3$  matrix  $W_L^i$  is computed to be:

$$Y^i Y^{i\dagger} = \begin{pmatrix} \frac{v^2}{2}|\lambda_{23}^i|^2 & \frac{v^2}{2}\lambda_{23}^i\lambda_{33}^{i*} & \frac{v^2}{2}\lambda_{23}^i\Lambda^{i*} \\ \frac{v^2}{2}\lambda_{23}^{i*}\lambda_{33}^i & \frac{v^2}{2}|\lambda_{33}^i|^2 + m^2 & \frac{v^2}{2}\lambda_{33}^i\Lambda^{i*} + mM^* \\ \frac{v^2}{2}\lambda_{23}^{i*}\Lambda^i & \frac{v^2}{2}\lambda_{33}^{i*}\Lambda^i + m^*M & \frac{v^2}{2}|\Lambda^i|^2 + M^2 \end{pmatrix} \quad (22)$$

Due to the same reasons as for  $W_R^i$  matrix perturbation theory can be applied.

$$W_L^i = \begin{pmatrix} 1 & W_{12}^{L,i} & W_{13}^{L,i} \\ -W_{12}^{L,i*} & 1 & W_{23}^{L,i} \\ -W_{13}^{L,i*} & -W_{23}^{L,i*} & 1 \end{pmatrix} \quad (23)$$

$$W_{12}^{L,i} = \frac{\frac{v^2}{2}\lambda_{23}^i\lambda_{33}^{i*}}{m^2 + \frac{v^2}{2}(|\lambda_{33}^i|^2 - |\lambda_{23}^i|^2)}$$

$$W_{13}^{L,i} = \frac{\frac{v^2}{2}\lambda_{23}^i\Lambda^{i*}}{M^2 + \frac{v^2}{2}(|\Lambda^i|^2 - |\lambda_{23}^i|^2)}$$

$$W_{23}^{L,i} = \frac{\frac{v^2}{2}\lambda_{33}^i\Lambda^{i*} + mM^*}{M^2 - m^2 + \frac{v^2}{2}(|\Lambda^i|^2 - |\lambda_{33}^i|^2)}$$

## 5.2 Parameter reduction

The physical effects of the mass mixing can be seen in vertices where different kind of fermions interact. In the SM such flavor changing effects only arise due to the charged current weak interaction with the  $W$ -boson and are described using the CKM-matrix.

$$\mathcal{L} \supset -i\frac{g_2}{\sqrt{2}}(\bar{u}_L\mathcal{W}^+W_L^{u\dagger}W_L^d d_L + \bar{u}_R\mathcal{W}^+W_R^{u\dagger}diag(0,1)W_R^d d_R + \bar{d}_L\mathcal{W}^-W_L^{d\dagger}W_L^u u_L + \bar{d}_R\mathcal{W}^-W_R^{d\dagger}diag(0,1)W_R^u u_R) \quad (24)$$

The CKM-matrix in the SM describes the flavour changing properties of the weak vertex.

$$\mathcal{L} \supset \bar{u}_L^{SM}\mathcal{W}^+V_{CKM}d_L^{SM} + \bar{d}_L^{SM}\mathcal{W}^-V_{CKM}^\dagger u_L^{SM} \quad (25)$$

Where  $u_L^{SM}$  and  $d_L^{SM}$  are vectors containing the three up-/down-type quark generations of the SM respectively. The elements of this matrix have been measured and can therefore be used to reduce the numbers of free parameters in this model [11]. The bottom right  $2 \times 2$ -matrix of  $V_{CKM}$  should then be equal to the upper-left  $2 \times 2$ -matrix of  $V_{4321} = W_L^{u\dagger}W_L^d$ .

$$V_{4321} = \begin{pmatrix} 1 + W_{12}^{L,u}W_{12}^{L,d*} + W_{13}^{L,u}W_{13}^{L,d*} & W_{12}^{L,d} - W_{12}^{L,u} + W_{13}^{L,u}W_{23}^{L,d*} & W_{13}^{L,d} - W_{13}^{L,u} - W_{12}^{L,u}W_{23}^{L,d} \\ W_{12}^{L,u*} - W_{12}^{L,d*} + W_{23}^{L,u}W_{13}^{L,d*} & 1 + W_{12}^{L,u*}W_{12}^{L,d} + W_{23}^{L,u}W_{23}^{L,d*} & W_{23}^{L,d} - W_{23}^{L,u} + W_{12}^{L,u*}W_{13}^{L,d} \\ W_{13}^{L,u*} - W_{13}^{L,d*} - W_{23}^{L,u*}W_{12}^{L,d*} & W_{23}^{L,u*} - W_{23}^{L,d*} + W_{13}^{L,u*}W_{12}^{L,d} & 1 + W_{13}^{L,u*}W_{13}^{L,d} + W_{23}^{L,u*}W_{23}^{L,d} \end{pmatrix} \quad (26)$$

The upper-left  $2 \times 2$  part of  $V_{4321}$  can be simplified using the Yukawa hierarchy  $\lambda_{23}^i \ll \lambda_{33}^i, \Lambda^i$ . These hierarchy assumptions are particularly well justified for the quark sector with its small mass mixing and ascending masses for later generations in the SM.

$$\begin{aligned}
W_{12}^{L,i} &: \mathcal{O}\left(\frac{\lambda_{23}^i}{\lambda_{33}^i}\right) \\
W_{13}^{L,i} &: \mathcal{O}\left(\frac{v^2}{M^2}\right) \\
W_{23}^{L,i} &: \mathcal{O}\left(\frac{m}{M}\right) \\
W_{12}^{R,i} &: \mathcal{O}\left(\frac{v}{M}\right)
\end{aligned} \tag{27}$$

It is assumed that the factors  $\frac{\lambda_{23}^i}{\lambda_{33}^i}$ ,  $\frac{m}{M}$  and  $\frac{v}{M}$  have a similar level of suppression and that  $m$  and  $v$  are of similar order. The upper-left  $2 \times 2$  part of  $V_{4321}$  is approximated up to  $\mathcal{O}\left(\frac{m}{M}/\frac{\lambda_{23}^i}{\lambda_{33}^i}\right)$ :

$$V_{4321} \approx \begin{pmatrix} 1 & W_{12}^{L,d} - W_{12}^{L,u} \\ W_{12}^{L,u*} - W_{12}^{L,d*} & 1 \end{pmatrix} \tag{28}$$

Looking at the Wolfenstein parametrization [12], it can be seen that at this level of accuracy this only yields one restriction on the parameters.

$$V_{CB} = W_{12}^{L,d} - W_{12}^{L,u} \tag{29}$$

Additional parameters can be eliminated by using the measurements of the top- and bottom-quark.

$$\begin{aligned}
Y_{diag}^i &= W_L^{i\dagger} Y^i W_R^i \\
&\Rightarrow \\
m_t &= \frac{v}{\sqrt{2}} \lambda_{23}^u W_{12}^{L,u*} + \frac{v}{\sqrt{2}} \lambda_{33}^u - m W_{12}^{R,u*} - \frac{v}{\sqrt{2}} \Lambda^u W_{23}^{L,u} + M W_{23}^{L,u} W_{12}^{R,u*} \\
m_b &= \frac{v}{\sqrt{2}} \lambda_{23}^d W_{12}^{L,d*} + \frac{v}{\sqrt{2}} \lambda_{33}^d - m W_{12}^{R,d*} - \frac{v}{\sqrt{2}} \Lambda^d W_{23}^{L,d} + M W_{23}^{L,d} W_{12}^{R,d*}
\end{aligned} \tag{30}$$

One can see that only the second term is not suppressed by the mass/Yukawa hierarchy and therefore it dominates. Additionally, the hypothesis is made that the mixed Yukawa coupling  $\lambda_{23}^d$  is equal to zero. This is done in order to get rid of all the couplings involving the first three generations, such that only the new mass parameters ( $m, M, \Lambda^u$  and  $\Lambda^d$ ) involving the fourth generation remain.

$$\begin{aligned}
\lambda_{33}^u &= \frac{m_t \sqrt{2}}{v} \\
\lambda_{33}^d &= \frac{m_b \sqrt{2}}{v} \\
V_{CB} = W_{12}^{L,u} &\Leftrightarrow \lambda_{23}^u = \frac{\sqrt{2} V_{CB} (|m|^2 + m_t^2)}{v m_t}
\end{aligned} \tag{31}$$

## Part III

 $U$ -quark decay

## 6 Decay widths

## 6.1 2-body decay

The transition amplitude for the two-body decay can be deduced from equation 24. This amplitude also has a right-handed contribution due to the  $SU(2)$  charge of the fourth generation.

$$iT = -\frac{ig_2}{2\sqrt{2}} \left( V_{4321}^{Ub} \bar{u}(p_2) \gamma^\mu (1 - \gamma_5) u(p_1) \epsilon_\mu^*(p_3) - W_{12}^{R,d*} \bar{u}(p_2) \gamma^\mu (1 + \gamma_5) u(p_1) \epsilon_\mu^*(p_3) \right) \quad (32)$$

The calculation of the decay width is done in good approximation with the simplifications  $m_W = 0$  and  $m_b = 0$ , as their masses should be negligible in comparison to the  $U$ -quark mass. The squared amplitude can then be summed over spin polarization and color final states and averaged over the initial state configurations.

$$\begin{aligned} \sum_{spin,col} T^\dagger T &= \frac{g_2^2}{16} \left( -\eta_{\mu\nu} - \frac{p_{3\mu} p_{3\nu}}{(p_3 \cdot n)^2} + \frac{p_{3\mu} n_\nu + p_{3\nu} n_\mu}{p_3 \cdot n} \right) p_{1\rho} p_{2\sigma} \cdot \\ &\left( |V_{4321}^{Ub}|^2 \left( 8(\eta^{\mu\sigma} \eta^{\nu\rho} - \eta^{\mu\nu} \eta^{\sigma\rho} + \eta^{\mu\rho} \eta^{\sigma\nu}) - 8i\epsilon^{\nu\rho\mu\sigma} \right) \right. \\ &\left. + |W_{12}^{R,d}|^2 \left( 8(\eta^{\mu\sigma} \eta^{\nu\rho} - \eta^{\mu\nu} \eta^{\sigma\rho} + \eta^{\mu\rho} \eta^{\sigma\nu}) + 8i\epsilon^{\nu\rho\mu\sigma} \right) \right) \quad (33) \\ n &= \begin{pmatrix} 1 \\ 0 \\ 0 \\ 0 \end{pmatrix} \quad p_1 = \begin{pmatrix} m_u \\ 0 \\ 0 \\ 0 \end{pmatrix} \quad p_2 = \begin{pmatrix} p \\ -\vec{p} \end{pmatrix} \quad p_3 = \begin{pmatrix} p \\ \vec{p} \end{pmatrix} \end{aligned}$$

While the terms with the metric tensor yield scalar products between the four momenta, the terms with the Levi-Civita tensor are harder to handle.  $n$  and  $p_1$  have all space-like coordinates equal to zero, which lets most terms including a factor of the Levi-Civita tensor go to zero. This is however not clear for the terms including the factor  $\frac{p_{3\mu} p_{3\nu}}{(p_3 \cdot n)^2}$ . Since  $p_1$  has to be taken with the index 0 for a term to be non-zero, the remaining factor is a (negative) product of the three entries of  $\vec{p}$ . For every Levi-Civita tensor, there are 6 such possibilities of which 3 are even and 3 are odd. Therefore, these terms cancel and it is sufficient to look at terms without a factor  $\epsilon^{\nu\rho\mu\sigma}$ .

Evaluating the scalar products and doing the phase space integral [13], yields:

$$\Gamma_{U \rightarrow Wb} = \frac{g_2^2 m_U}{32\pi} (|V_{4321}^{Ub}|^2 + |W_{12}^{R,d}|^2) \quad (34)$$

Rewriting this in terms of the initial mass parameters, one gets:

$$\begin{aligned} m_U &= W_{13}^{L,u*} W_{12}^{R,u} \lambda_{23}^u \frac{v}{\sqrt{2}} + W_{23}^{L,u*} \frac{v}{\sqrt{2}} \lambda_{33}^u W_{12}^{R,u} + W_{23}^{L,u*} m + \frac{v}{\sqrt{2}} \Lambda^u W_{12}^{R,u} + M \approx M \\ |V_{4321}^{Ub}|^2 &\approx \frac{m_t^2 v^2 |\Lambda^u|^2}{2M^4} + \frac{m_b^2 v^2 |\Lambda^d|^2}{2M^4} - \frac{2\text{Re}(m_t m_b^* v^2 \Lambda^{u*} \Lambda^d)}{2M^4} \\ |W_{12}^{R,d}|^2 &\approx \frac{v^2 M^2 |\Lambda^d|^2}{2M^4} + \frac{m^2 m_b^2}{M^4} + \frac{\sqrt{2} v \text{Re}(m^* M m_b \Lambda^{d*})}{M^4} \end{aligned} \quad (35)$$

The leading order contribution from  $|V_{4321}^{Ub}|^2$  cancels. This renders the left-handed contribution to be suppressed compared to the decay with a right-handed vertex and therefore only the right-handed vertex contributes at leading and next-to-leading order. When the suppressed highest-order (next-to-next-to-leading order) terms are neglected, the decay width of this two-body decay is given by.

$$\Gamma_{U \rightarrow Wb} = \frac{g_2^2 M}{32\pi} \left( \frac{v^2 M^2 |\Lambda^d|^2}{2M^4} + \frac{\sqrt{2} v \operatorname{Re}(m^* M m_b \Lambda^{d*})}{M^4} \right) \quad (36)$$

Note that there are no contributions from the left-handed vertices to this accuracy.

## 6.2 3-body decay

As a next step, the decay width of the 3-body decay is to be found. Again, all particles in the final state are assumed to be massless. For this, the Effective Field Theory (EFT) framework is used [14], where it is assumed that the mass of the Leptoquark  $m_{LQ}$  is much larger than the  $U$ -quark mass, giving rise to 6-dimensional operators. The Leptoquark part of the Lagrangian has already been shown in equation 3. To see the flavor structure of these vertices better, these interaction vertices have to be written using the multiplets which were introduced in section 5.

$$\begin{aligned} \mathcal{L} \supset -\frac{ig_A}{\sqrt{3}} & \left( \bar{u}_L W_L^{u\dagger} \text{diag}(0, \Psi^+, \Psi^+) W_L^\nu \nu_L + \bar{d}_L W_L^{d\dagger} \text{diag}(0, \Psi^+, \Psi^+) W_L^e e_L \right. \\ & + \bar{\nu}_L W_L^{\nu\dagger} \text{diag}(0, \Psi^-, \Psi^-) W_L^u u_L + \bar{e}_L W_L^{e\dagger} \text{diag}(0, \Psi^-, \Psi^-) W_L^d d_L \\ & + \bar{u}_R W_R^{u\dagger} \text{diag}(\Psi^+, 0) W_R^\nu \nu_R + \bar{d}_R W_R^{d\dagger} \text{diag}(\Psi^+, 0) W_R^e e_R \\ & \left. + \bar{\nu}_R W_R^{\nu\dagger} \text{diag}(\Psi^-, 0) W_R^u u_R + \bar{e}_R W_R^{e\dagger} \text{diag}(\Psi^-, 0) W_R^d d_R \right) \quad (37) \end{aligned}$$

It is interesting to take a closer look at the flavor structure of the process.

$$\begin{aligned} W_L^{i\dagger} \text{diag}(0, \Psi, \Psi) W_L^j &= \\ \Psi \begin{pmatrix} W_{12}^{i,L} W_{12}^{j,L*} + W_{13}^{i,L} W_{13}^{j,L*} & W_{13}^{i,L} W_{23}^{j,L*} - W_{12}^{i,L} & -W_{13}^{i,L} - W_{12}^{i,L} W_{23}^{j,L} \\ W_{23}^{i,L} W_{13}^{j,L*} - W_{12}^{j,L*} & 1 + W_{23}^{i,L} W_{23}^{j,L*} & W_{23}^{j,L} - W_{23}^{i,L} \\ -W_{13}^{j,L*} - W_{23}^{i,L*} W_{12}^{j,L*} & W_{23}^{i,L*} - W_{23}^{j,L*} & 1 + W_{23}^{i,L*} W_{23}^{j,L} \end{pmatrix} \quad (38) \\ W_R^{i\dagger} \text{diag}(\Psi, 0) W_R^j &= \Psi \begin{pmatrix} 1 & W_{12}^{j,R} \\ W_{12}^{i,R*} & W_{12}^{i,R*} W_{12}^{j,R} \end{pmatrix} \end{aligned}$$

These matrices are particularly interesting when one decides which flavors of neutrinos are considered in the final state. One can see that the largest contribution in the left-handed part is coming from the diagonal element, while for the right-handed vertices a decay into the  $\nu_\tau$  seems to be favored. The decay into  $\nu_\mu$  is more heavily suppressed and is therefore neglected in this thesis.

### 6.2.1 Wilson coefficients

In this chapter the EFT framework will be used to approximate the decay width for large Leptoquark masses.

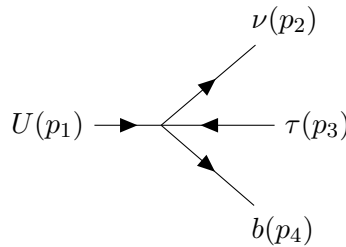


Figure 2: Feynman diagram of a 6-dimensional EFT operator describing the  $U$ -quark decay.

Using the Feynman gauge, one can predict the Dirac structure of these vertices. The different right- and left-handed vertices in the full theory have to be accounted for too. Since the leading order in the EFT power counting is the desired accuracy for this thesis, only the following terms



from the EFT Lagrangian are relevant for the  $U$ -quark decay.

$$\begin{aligned} \mathcal{L}_{EFT} \supset & \frac{C_L^\tau}{\Lambda^2} (\bar{U}_L \gamma^\mu \nu_L^\tau \bar{\tau}_L \gamma_\mu b_L) + \frac{C_{LR}^\tau}{\Lambda^2} (\bar{U}_L \gamma^\mu \nu_L^\tau \bar{\tau}_R \gamma_\mu b_R) \\ & + \frac{C_{RL}^\tau}{\Lambda^2} (\bar{U}_R \gamma^\mu \nu_R^\tau \bar{\tau}_L \gamma_\mu b_L) + \frac{C_R^\tau}{\Lambda^2} (\bar{U}_R \gamma^\mu \nu_R^\tau \bar{\tau}_R \gamma_\mu b_R) + \frac{C_L^N}{\Lambda^2} (\bar{U}_L \gamma^\mu N_L \bar{\tau}_L \gamma_\mu b_L) \\ & + \frac{C_{LR}^N}{\Lambda^2} (\bar{U}_L \gamma^\mu N_L \bar{\tau}_R \gamma_\mu b_R) + \frac{C_{RL}^N}{\Lambda^2} (\bar{U}_R \gamma^\mu N_R \bar{\tau}_L \gamma_\mu b_L) + \frac{C_R^N}{\Lambda^2} (\bar{U}_R \gamma^\mu N_R \bar{\tau}_R \gamma_\mu b_R) \end{aligned} \quad (39)$$

The tree-level four-point function  $iT_{EFT}(U \rightarrow \nu\tau b)$ , that arises from these EFT terms up to order  $\Lambda^2$ , has to be equal to the tree-level four-point function of the full theory up to order  $\frac{1}{m_{LQ}^2}$ . From equation 37 the Feynman rules and subsequently the full theory four-point function can be deduced. During this step the Leptoquark propagator has to be rewritten in order to get a power counting.

$$\begin{aligned} \frac{-i\eta_{\mu\nu}}{(p_1 - p_2)^2 - m_{LQ}^2} &= \frac{i\eta_{\mu\nu}}{m_{LQ}^2} \left[ 1 + \frac{(p_1 - p_2)^2}{m_{LQ}^2} + \mathcal{O}\left(\left(\frac{(p_1 - p_2)^2}{m_{LQ}^2}\right)^2\right) \right] \\ (p_1 - p_2)^2 &= m_U^2 - 2m_U |p_2| \end{aligned} \quad (40)$$

$|p_2|$  denotes the magnitude of the neutrino momentum in the center-of-mass frame of the  $U$ -quark and is bound from above at  $|p_2| = \frac{m_U}{2}$  due to energy conservation.

By setting equal the four-point functions, the tree level matching for the Wilson coefficients can easily be read out.

$$\begin{aligned} \Lambda &= m_{LQ} \\ C_L^\tau &= -\frac{ig_4^2}{3} (W_{23}^{u,L*} - W_{23}^{\nu,L*}) (1 + W_{23}^{e,L} W_{23}^{d,L*}) \\ C_{LR}^\tau &= -\frac{ig_4^2}{3} (W_{23}^{u,L*} - W_{23}^{\nu,L*}) \\ C_{RL}^\tau &= -\frac{ig_4^2}{3} W_{12}^{u,R*} (1 + W_{23}^{e,L} W_{23}^{d,L*}) \\ C_R^\tau &= -\frac{ig_4^2}{3} W_{12}^{u,R*} \\ C_L^N &= -\frac{ig_4^2}{3} (1 + W_{23}^{u,L*} W_{23}^{\nu,L}) (1 + W_{23}^{e,L} W_{23}^{d,L*}) \\ C_{LR}^N &= -\frac{ig_4^2}{3} (1 + W_{23}^{u,L*} W_{23}^{\nu,L}) \\ C_{RL}^N &= -\frac{ig_4^2}{3} W_{12}^{u,R*} W_{12}^{\nu,R} (1 + W_{23}^{e,L} W_{23}^{d,L*}) \\ C_R^N &= -\frac{ig_4^2}{3} W_{12}^{u,R*} W_{12}^{\nu,R} \end{aligned} \quad (41)$$

$$\begin{aligned} iT_{EFT}(U \rightarrow \nu\tau b) &= \frac{1}{4m_{LQ}^2} \left( (C_L^\tau + C_L^N) \bar{u}(p_2) \gamma^\mu (1 - \gamma_5) u(p_1) \bar{u}(p_4) \gamma_\mu (1 - \gamma_5) v(p_3) \right. \\ &+ (C_{LR}^\tau + C_{LR}^N) \bar{u}(p_2) \gamma^\mu (1 - \gamma_5) u(p_1) \bar{u}(p_4) \gamma_\mu (1 + \gamma_5) v(p_3) \\ &+ (C_{RL}^\tau + C_{RL}^N) \bar{u}(p_2) \gamma^\mu (1 + \gamma_5) u(p_1) \bar{u}(p_4) \gamma_\mu (1 - \gamma_5) v(p_3) \\ &\left. + (C_R^\tau + C_R^N) \bar{u}(p_2) \gamma^\mu (1 + \gamma_5) u(p_1) \bar{u}(p_4) \gamma_\mu (1 + \gamma_5) v(p_3) \right) \end{aligned} \quad (42)$$

Note that  $\bar{u}(p_2)$  are technically different for Wilson coefficients with different index  $\tau/N$ . They are put as the same here nevertheless, since both neutrinos  $\nu^\tau$  and  $N$  are approximated to be

massless and thus have the same properties for this calculation.

A long calculation yields the following for the squared amplitude, which is summed over final spin states and averaged over initial spin states. Note that for the decays analyzed in this thesis the color summation gives a factor 1, since there are no color changing vertices involved.

$$\begin{aligned} \sum_{spin,col} \bar{|T|^2} = \frac{8}{m_{LQ}^4} & \left( \left( |C_L^\tau|^2 + |C_L^N|^2 + |C_R^\tau|^2 + |C_R^N|^2 + 2Re(C_L^{\tau*} C_L^N) + 2Re(C_R^{\tau*} C_R^N) \right) (p_1 p_4)(p_2 p_3) \right. \\ & \left. + \left( |C_{LR}^\tau|^2 + |C_{LR}^N|^2 + |C_{RL}^\tau|^2 + |C_{RL}^N|^2 + 2Re(C_{LR}^{\tau*} C_{LR}^N) + 2Re(C_{RL}^{\tau*} C_{RL}^N) \right) (p_1 p_3)(p_2 p_4) \right) \end{aligned} \quad (43)$$

### 6.2.2 Phase space

Finally, it remains to do the phase space integral [15]. Below there is the connection between the decay width and the squared transition amplitude [13].

$$d\Gamma = \frac{(2\pi)^4}{2m_U} \sum_{spin,col} \bar{|T|^2} \delta^4(p_1 - p_2 - p_3 - p_4) \frac{d^3 p_2 d^3 p_3 d^3 p_4}{8(2\pi)^9 E_2 E_3 E_4} \quad (44)$$

For this integration it is useful to realize that the final state particles are on a plane in the rest frame of the decaying particle. Therefore, the first angular integration around the  $z$ -axis can already be done.

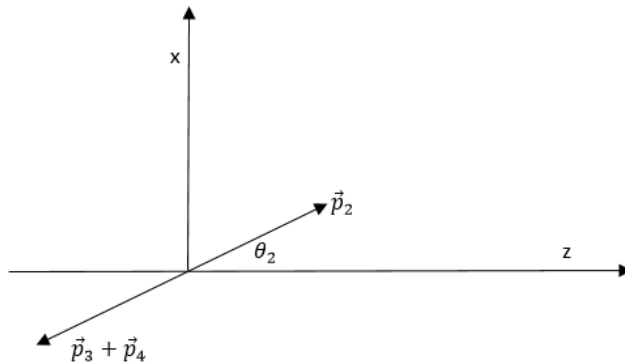


Figure 3: Schematic figure of the 3-body decay in the rest frame of the  $U$ -quark.

$$\begin{aligned} \Gamma &= \frac{2\pi}{(2\pi)^5 4m_U} \int_{-1}^1 d\cos(\theta_2) \int_0^{\frac{m_U}{2}} d|p_2| |p_2| \int \frac{d^3 p_3 d^3 p_4}{4|p_3| |p_4|} \sum_{spin,col} \bar{|T|^2} \delta^4(p_1 - p_2 - p_3 - p_4) \\ U &= \int \frac{d^3 p_3 d^3 p_4}{4|p_3| |p_4|} \sum_{spin,col} \bar{|T|^2} \delta^4(p_1 - p_2 - p_3 - p_4) \end{aligned} \quad (45)$$

The last part of the integral  $U$  is Lorentz invariant and can therefore be evaluated in the center-of-mass frame of the  $b$ -quark and the tauon. Performing this integration and thus eliminating

the Dirac distribution, yields:

$$\begin{aligned}\Gamma &= \frac{1}{4(2\pi)^4 m_U} \int_0^{\frac{m_U}{2}} dp_2 p_2 \int_{-1}^1 d\cos(\theta_2) \int_{-1}^1 d\cos(\theta^*) \int_0^{2\pi} d\phi^* \left( a(p_1 p_3)(p_2 p_4) + b(p_1 p_4)(p_2 p_3) \right) \\ a &= \frac{1}{m_{LQ}^4} (|C_{LR}^\tau|^2 + |C_{LR}^N|^2 + |C_{RL}^\tau|^2 + |C_{RL}^N|^2 + 2\text{Re}(C_{LR}^{\tau*} C_{LR}^N) + 2\text{Re}(C_{RL}^{\tau*} C_{RL}^N)) \\ b &= \frac{1}{m_{LQ}^4} (|C_L^\tau|^2 + |C_L^N|^2 + |C_R^\tau|^2 + |C_R^N|^2 + 2\text{Re}(C_L^{\tau*} C_L^N) + 2\text{Re}(C_R^{\tau*} C_R^N))\end{aligned}\tag{46}$$

The four-momenta used for this calculation are shown next. Note that the vectors  $p_3^*$  and  $p_4^*$  are in the center-of-mass frame of the  $b$ -quark and  $\tau$ . Accordingly they have to be rotated around the  $y$ -axis with angle  $(\theta_2 + \pi)$  and boosted along the  $z$ -axis with  $\gamma = \frac{m_u - |p_2|}{m_{12}}$  to get into the rest frame of the  $U$ -quark.

$$\begin{aligned}p_1 &= \begin{pmatrix} m_U \\ 0 \\ 0 \\ 0 \end{pmatrix} \quad p_2 = |p_2| \begin{pmatrix} 1 \\ \sin(\theta_2) \\ 0 \\ \cos(\theta_2) \end{pmatrix} \quad p_3^* = \frac{m_{12}}{2} \begin{pmatrix} 1 \\ \sin(\theta^*) \cos(\phi^*) \\ \sin(\theta^*) \sin(\phi^*) \\ \cos(\theta^*) \end{pmatrix} \\ p_4^* &= \frac{m_{12}}{2} \begin{pmatrix} 1 \\ -\sin(\theta^*) \cos(\phi^*) \\ -\sin(\theta^*) \sin(\phi^*) \\ -\cos(\theta^*) \end{pmatrix} \quad m_{12} = \sqrt{m_U^2 - 2m_U |p_2|}\end{aligned}\tag{47}$$

The final result for the decay width is then attained by performing the remaining integrals.

$$\Gamma_{U \rightarrow \nu \tau b} = \frac{(a+b)m_U^5}{(2\pi)^3 192}\tag{48}$$

The full expression can then be found by evaluating and expanding the variables  $a$  and  $b$  using the mass and Yukawa hierarchy. Again, equation 35 is used to approximate the  $U$ -quark mass using the Yukawa and mass parameters. Since the next-to-leading order vanishes, only the leading order contribution is stated here:

$$\Gamma_{U \rightarrow \nu \tau b} = \frac{g_4^4 M^5}{(2\pi)^3 864 m_{LQ}^4}\tag{49}$$

It is also interesting to study where the leading order contributions for the decay width are coming from:

$$\begin{aligned}a &= \frac{1}{m_{LQ}^4} (|C_{LR}^\tau|^2 + |C_{LR}^N|^2 + |C_{RL}^\tau|^2 + |C_{RL}^N|^2 + 2\text{Re}(C_{LR}^{\tau*} C_{LR}^N) + 2\text{Re}(C_{RL}^{\tau*} C_{RL}^N)) \\ &\stackrel{\text{LO}}{=} \frac{1}{m_{LQ}^4} (|C_{LR}^N|^2)_{LO} \\ b &= \frac{1}{m_{LQ}^4} (|C_L^\tau|^2 + |C_L^N|^2 + |C_R^\tau|^2 + |C_R^N|^2 + 2\text{Re}(C_L^{\tau*} C_L^N) + 2\text{Re}(C_R^{\tau*} C_R^N)) \\ &\stackrel{\text{LO}}{=} \frac{1}{m_{LQ}^4} (|C_L^N|^2)_{LO}\end{aligned}\tag{50}$$

One can see that the leading order contribution stems from the decay into a fourth generation neutrino.

## 7 The ratio $R$

Finally, all ingredients are ready to express the  $R$  ratio using the leading order contribution from the two different  $U$ -quark decay widths. This leads to the following quantity for  $R$ :

$$R = \frac{108g_2^2v^2|\Lambda^d|^2\pi^2m_{LQ}^4}{g_4^4m_U^6} \quad (51)$$

Here, the fact has been used that the  $U$ -quark mass is equal to the mass parameter  $M$  in a good approximation (see equation 35).

It is particularly interesting to look which decay channel dominates at which range of our mass parameters. Since we have assumed that  $m_U < m_{LQ}$  in our calculation, the  $U$ -quark mass can be parametrised in the following way using an  $\epsilon$  between  $0 < \epsilon < 1$ .

$$m_U = \epsilon m_{LQ} \quad (52)$$

Using this parametrization, the value  $\epsilon_0$ , where the two decay widths are the same, can be found. For  $\epsilon > \epsilon_0$  the 3-body decay width is larger than the two-body decay width. For  $\epsilon < \epsilon_0$  the reverse is the case.

$$\epsilon_0 = \left( \frac{g_2^2v^2|\Lambda^d|^2\pi^2108}{g_4^4m_{LQ}^2} \right)^{\frac{1}{6}} \approx 0.27 \left( \frac{\Lambda^d}{0.1} \right)^{\frac{1}{3}} \left( \frac{3}{g_4} \right)^{\frac{2}{3}} \left( \frac{3TeV}{m_{LQ}} \right)^{\frac{1}{3}} \quad (53)$$

It is obvious that  $\epsilon_0$  is suppressed by our mass hierarchy, since we have assumed  $m_{LQ} > m_U \approx M$ . Nevertheless, this is not a large suppression, since the exponent yields that  $\epsilon_0$  is only proportional to  $\left( \frac{v}{m_{LQ}} \right)^{\frac{1}{3}}$ . The only Yukawa factor in this equation is the mixing parameter  $\Lambda^d$  between the fourth and third generation. When this mixing parameter is increased, it enlarges the range in which the 2-body decay dominates. This does not come as a surprise, since only the 2-body decay mode is dependent on flavor changing vertices at leading order. Furthermore, a numerical reference value was found for  $\epsilon_0$  using natural guesses for the  $SU(4)$  parameters:  $m_{LQ} = 3 TeV$ ,  $g_4 = 3$  and  $\Lambda^d = 10^{-1}$ . For this numerical example, the  $U$ -quark mass at which the two decay modes have the same strength is approximately 810 GeV. To get that numerical result, the following values were used for the SM parameters  $g_2$  and  $v$ .

$$g_2 = 6.5 \cdot 10^{-1} \quad v = 246 GeV \quad (54)$$

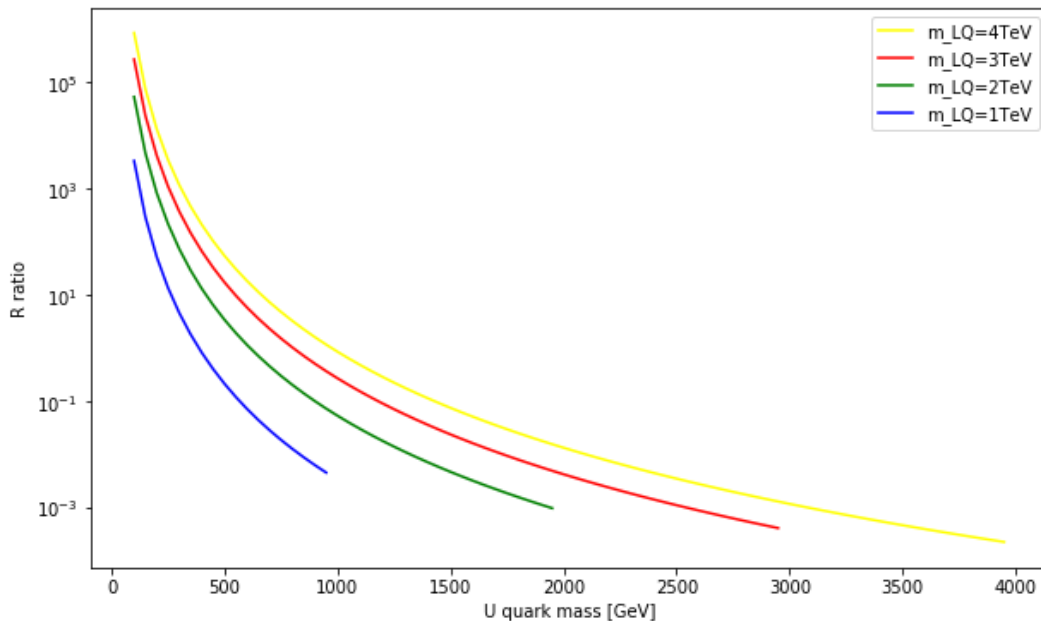


Figure 4:  $R$  ratio as a function of the  $U$ -quark mass for different LQ masses.

It is interesting as well to plot  $R$  as a function of the  $U$ -quark mass. Again, the plots were evaluated with the values from equation 54 and with the parameter values  $g_4 = 3$  and  $\Lambda^d = 10^{-1}$ . In figure 4  $R$  is plotted for different masses of the Leptoquark  $m_{LQ}$ . As expected for a fixed mass of the Leptoquark  $m_{LQ}$ , the 3-body decay channel gains relative strength with respect to the weak decay when the  $U$ -quark mass  $m_U$  is increased. However, it is important to note that this only represents the leading order contributions from the EFT. Due to the large coupling constant  $g_4 = 3$ , the EFT power counting competes with the coupling strength. For large  $U$ -quark masses ( $m_U \rightarrow m_{LQ}$ ), the EFT cannot be handled perturbatively anymore (see equation 40). Thus, the leading order contribution depicted in figure 4 gets less relevant for larger masses  $m_U$ .

Finally, one can define a mass  $m_{U,0} = \epsilon_0 m_{LQ}$  corresponding to the  $U$  quark mass at which the decay widths of the two modes are the same. Equation 53 states that the factor  $\epsilon_0$  increases when the Leptoquark mass  $m_{LQ}$  is decreased. However, this is only relative to the Leptoquark mass  $m_{LQ}$ , which is not fixed itself. It is therefore interesting to see how the corresponding mass  $m_{U,0}$  changes. In the plots in figure 4 that change can be easily seen. The mass  $m_{U,0}$  increases with an increasing Leptoquark mass, even though it gets relatively smaller compared to  $m_{LQ}$ .

## Part IV

# Conclusions & Outlook

4321 models are interesting, since they could give an explanation for the deviation to Standard Model predictions in B meson decays. In this thesis the decay of a fourth generation  $U$ -quark was studied for the 4321-framework. In the specific model that was chosen, the third and fourth generation behave differently and Lepton flavor-universality is only given approximately for low energies. Using assumptions about the mass hierarchy and neglecting small masses, the decay widths for the two decay modes were computed separately up to next-to-leading order in the mass hierarchy. There is the decay mode involving the weak interaction ( $U \rightarrow Wb$ ) and the Leptoquark decay mode into three particles ( $U \rightarrow \nu b \tau$ ). The leading order decay widths were then compared using the ratio  $R$  between the two decay widths and  $R$  was plotted as a function of the  $U$ -quark mass for different Leptoquark masses.

As a next step, it would be interesting to calculate the decay widths with more orders in the mass hierarchy. Additionally, the ratio  $R$  could also be analyzed using more orders in the decay widths and thus getting a more exact result. Furthermore, not neglecting the small masses ( $m_W, m_b, m_\tau$  and  $m_\nu$ ) in the decay width calculations would also increase the accuracy of this analysis.

Finally, it is also important to retain the connection to the experiments. Consequently, the anomalies in flavor physics should be studied further in experiments and more data on this subject is needed to get statistically more significant results. By studying the  $B$ -meson decay and confirming or discarding the anomalies, the relevance of the 4321-models can be changed.

## References

- [1] R. Oerter, The theory of almost everything: The Standard Model, the unsung triumph of modern physics, *Penguin Publishing Group*, (2006).
- [2] J.D. Lykken, Beyond the Standard Model, *High Energy Physics - Phenomenology*, (2010).
- [3] V. Barger, D. Marfatia and K. Whisnant, The Physics of Neutrinos, *Princeton University Press*, 2012.
- [4] S Amoroso, Precision measurements at the LHC, *PoS*, (2020).
- [5] LHCb Collaboration, P. de Simone, Experimental Review on Lepton Universality and Lepton Flavour Violation tests in B decays, *EPJ Web of Conferences* 234, 01004, (2020).
- [6] LHCb Collaboration, R. Aaij et al, Tests of Lepton Universality Using  $B^0 \rightarrow K_s^0 l^+ l^-$  and  $B^+ \rightarrow K^{*+} l^+ l^-$  Decays, *Physical Review Letters* 128, 191802 (2022).
- [7] BABAR Collaboration, J.P. Lees et al, Evidence for an Excess of  $\bar{B} \rightarrow D^{(*)} \tau^- \bar{\nu}_\tau$  Decays, *Physical Review Letters* 109, 101802 (2012).
- [8] G. Valencia and S.Willenbrock, Quark-lepton unification and rare meson decays, *Physical Review D* 50 , 6843 (1994).
- [9] J. Fuentes-Martin, G. Isidori, M. König and N.Selimovic, Vector Leptoquarks Beyond Tree Level III: Vector-like Fermions and Flavor-Changing Transitions, *High Energy Physics - Phenomenology*, (2020).
- [10] F. Kreuzer, Lower Bound on Mass of the Leptoquark in Pati-Salam Standard Model Extension, *Thesis at ETH*, (2018).
- [11] M. Tanabashi et al. (Particle Data Group), *Phys. Rev. D* 98, 030001, (2018).
- [12] L. Wolfenstein, Parametrization of the Kobayashi-Maskawa Matrix, *Physical Review Letters*, 51, 1945 – 1947, (1983).
- [13] P.A. Zyla et al. (Particle Data Group), Review of Particle Physics, *Progress of Theoretical and Experimental Physics*, 083C01, (2020).
- [14] A.V. Manohar, Effective Field Theories (Lectures), *High Energy Physics - Phenomenology*, (1995).
- [15] J. C. Romao, Integration of three body phase space: The 3BodyXSections and 3BodyDecays packages, Notes from series "Computational Techniques in Quantum Field Theory", *Instituto Superior Tecnico*, (2022).